The Variations of Photoluminscence Decay Times Under The Influence of A Trapping State

K. P. Chiu
Department of Physics
Chung Yuan Christian University
No. 200, Zhongbei Rd., Zhongli Dist., Taoyuan City 320314, Taiwan, R.O.C.
kpchiu@cycu.edu.tw

***Abstract*—We numerically calculated the time-resolved photoluminescence spectra using the bimolecular trapping-detrapping model. The variations of carrier lifetimes are investigated by changing the carrier recombination and trapping rate constants, as well as the concentration of available trapping states.**

Keywords—time-resolved photoluminescence, bimolecular trapping-detrapping model, triexponential decaying function

I. Introduction

Perovskite materials are recently attracted a lot of attentions in the research area of solar cell applications. Their outstanding intrinsic properties, such as high absorption coefficient [1], tunable band gap [2], large carrier diffusion-length [3] and carrier mobility [4], show the potential improvement in the photovoltaic performance of a solar cell. However, to the practical purpose in designing the optoelectronic device and improving its photovoltaic efficiency, it needs to understand the fundamental interactions between photons and the carriers in the material. Time-resolved photoluminescence (TRPL) spectroscopy is one of the powerful techniques to investigate the mechanism of electron transition processes in photoluminescence materials. In this work, we will numerically analyze and discuss the evolution of the excitonic and trap state electron populations in the perovskite material with respect to time using the bimolecular trapping-detrapping model [5]. From the results of time evolution populations, it is possible to imitate the TRPL spectra of the sample. The influence of different material parameters, such as the concentrations of excitonic and trapped carriers, the concentration of trap state, and the radiative and non-radiative carrier transition rates, on the behavior of TRPL can be systematically analyzed. These results can provide helpful information to understand the connection between the physical processes happened within the material and the observed TRPL spectra.

II. Numerical Calculation Model

In the following calculations, we consider the phenomenological model depicted in Fig. 1. There are two distinct states for electrons, the excited state and the trapping state. The total available concentration of the trapping state is N_T (cm^{-3}). The concentration of photo-generated electrons produced by illuminating a single pumping pulse is N_0 (cm^{-3}). After the illumination, some of the photo-generated electrons will be recombined with the holes in the valance band, and some of them will be transited and trapped into the trapping state. The time dependent concentrations of electrons in the excited and trap states are n_E (cm^{-3}) and n_T (cm^{-3}), respectively.

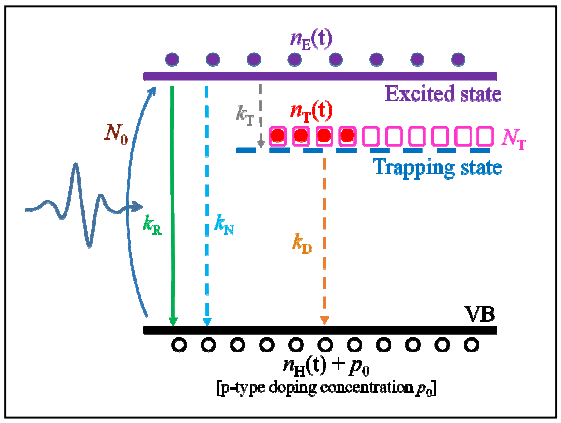

Fig. 1. Schematic diagram for describing the transition processes of the photoexcited carriers

And the associated time dependent concentration of photo-generated holes in the valance band is n_H (cm^{-3}). We consider the sample is positively doped with doping concentration p_0 (cm^{-3}). Therefore, the total concentration of holes in the valance band is $(n_H + p_0)$ after the pumping pulse.

The bimolecular trapping-detrapping model is used to describe the time rate of change of each carrier concentrations, which are described in the following set of equations.

$$dn_E/dt = -k_B n_E(n_H + p_0) - k_T n_E(N_T - n_T)$$
$$dn_H/dt = -k_B n_E(n_H + p_0) - k_D n_T(n_H + p_0) \quad (1)$$
$$dn_T/dt = +k_T n_E(N_T - n_T) - k_D n_T(n_H + p_0)$$

The rate constant k_B is the combination of radiative and non-radiative recombination rate constants, k_R and k_N. The electron trapping and detrapping rate constants are k_T and k_D, respectively. The fifth order Runge-Kutta method is used to solve (1) with initial values $n_E(0) = n_H(0) = N_0$, $n_T(0) = 0$ for various k_B, k_D, k_T and N_T values. To investigate the influence of the power of the pumping pulse, different values of N_0 is also used in our calculations. After solving the equations to obtain the time dependent n_E, n_H and n_T, the TRPL intensity is estimated by

$$I_{TRPL}(t) = k_R n_E(t)[n_H(t) + p_0)]. \quad (2)$$

The default parameters setting in the following calculations are $N_0 = 500\times10^{12}$ (cm^{-3}), $N_T = 60\times10^{12}$ (cm^{-3}), p_0

978-1-6654-7899-1/22/$31.00 ©2022 IEEE

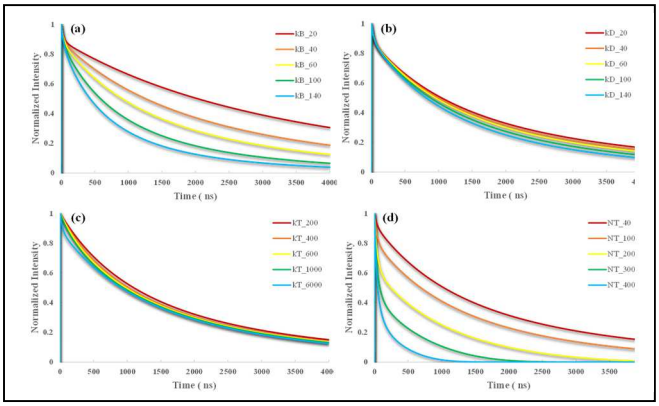

= 65×10^{12} (cm^{-3}), k_B = 60×10^{-20} (cm^3/ns), k_D = 80×10^{-20} (cm^3/ns), and $k_T = 6000\times10^{-20}$ (cm^3/ns). With changing single

Fig. 2. The cclculated TRPL spectra for (a) different k_B, (b) different k_D, (c) different k_T, and (d) different N_T.

parameter once a time, the TRPL spectra are calculated and their corresponding carrier lifetimes are analyzed.

III. Results And Discussion

The results shown in Fig. 2(a) to 2(d) are the calculated TRPL spectra using the default parameters but changing the value of k_B, k_D, k_T, and N_T, respectively. The increasing in k_B and N_T affect the TRPL spectra more obviously in full time duration of the calculation. And, the increasing in k_T and k_D mainly affect the behavior of TRPL spectra in the beginning and in the long-time duration of the calculation, respectively. To quantitatively analyze the carrier lifetimes, the TRPL spectra were fitted by a sum of three exponentially decaying functions $A_1\exp(-t/\tau_1) + A_2\exp(-t/\tau_2) + A_1\exp(-t/\tau_3)$.

The variations of carrier lifetimes with increasing k_B, k_D, and k_T are shown in Fig. 3. The long lifetime (τ_3) and medium lifetime (τ_2) gradually decrease with increasing k_B, but the short lifetime (τ_1) slightly increases from 35 ns to 40 ns. The increasing k_D results in slightly decreasing τ_2 and τ_3, and has almost no effect on τ_1 which remains at about 35 ns. With increasing k_T, all the three lifetimes rapidly decrease when k_T is smaller than 1000×10^{-20} (cm^3/ns). For even larger k_T, τ_1 remains gradually decreasing, but τ_2 and τ_3 are slightly increase.

IV. Conclusion

In this work, we numerically calculated the TRPL spectra using the bimolecular trapping-detrapping model for different recombination rate constants and concentration of available trapping state. The resulted TRPL spectra can be fitted by a triexponential decaying function to obtain three carrier lifetimes. The variation of the long and medium lifetimes with increasing k_B and k_T are similar, and the variation trend of the short lifetime has different behavior. The carrier lifetimes are relatively less sensitive to the change in k_D.

Acknowledgment

This work was supported by the Ministry of Science and Technology Taiwan under the Grant Nos. MOST 110-2112-M-033-012.

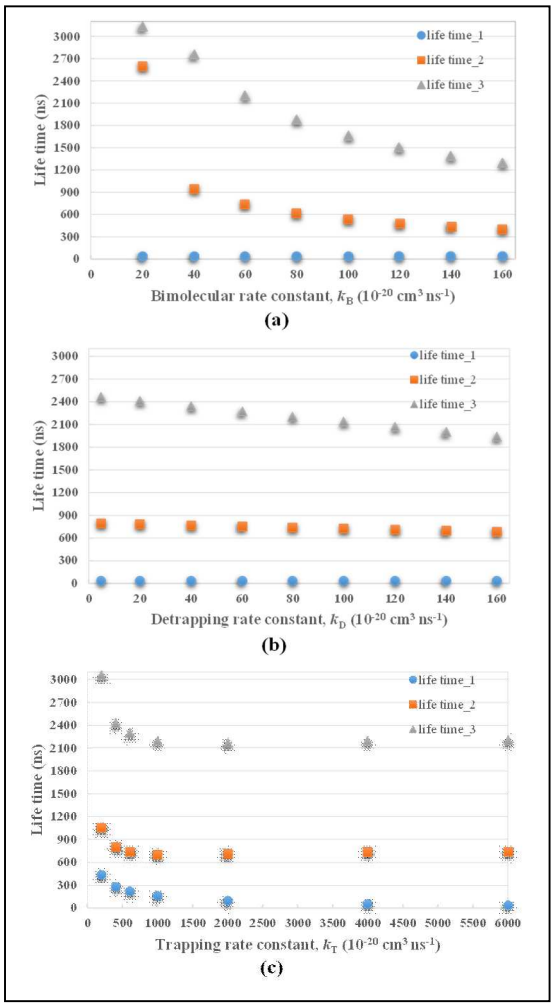

Fig. 3. The variation of carrier lifetimes with different k_B, k_D, and k_T.

References

[1] S. De Wolf, J. Holovsky, S.J. Moon, P. Loper, B. Niesen, et al., "Organometallic halide perovskites: sharp optical absorption edge and its relation to photovoltaic performance," *J. Phys. Chem. Lett.*, vol. 5, pp. 1035–1039, March 2014.

[2] J.H. Noh, S.H. Im, J.H. Heo, T.N. Mandal, and S.I. Seok, "Chemical management for colorful, efficient, and stable inorganic–organic hybrid nanostructured solar cells," *Nano Lett.*, vol. 13, pp. 1764–1769, March 2013.

[3] Q. Dong, Y. Fang, Y. Shao, P. Mulligan, J. Qiu, et al., "Electron-hole diffusion lengths > 175 μm in solution-grown $CH_3NH_3PbI_3$ single crystals," *Science*, vol. 347, pp. 967–970, Jan 2015.

[4] S.D. Stranks, G.E. Eperon, G. Grancini, C. Menelaou, M.J.P. Alcocer, et al., "Electron-hole diffusion lengths exceeding 1 micrometer in an organometal trihalide perovskite absorber," *Science*, vol. 342, pp. 341–344, Oct 2013.

[5] E.V. Péan, S. Dimitrov, C.S. De Castroc, and M. L. Davies, "Interpreting time-resolved photoluminescence of perovskite materials," *Phys. Chem. Chem. Phys.*, vol. 22, pp. 28345–28358, Nov 2020.